Three-dimensional proximity effect correction for large-scale uniform patterns

Q. Dai and S.-Y. Lee[a)]
Department of Electrical and Computer Engineering, Auburn University, Auburn, Alabama 36849

S.-H. Lee, B.-G. Kim, and H.-K. Cho
Samsung Electronics, Photomask Division, 16 Banwol-Dong, Hwasung, Kyunggi-Do, Korea

(Received 29 June 2011; accepted 21 October 2011; published 18 November 2011)

One of the major limiting factors in electron beam (e-beam) lithography is the geometric distortion of written features due to electron scattering, which is known as the proximity effect. A conventional approach to the proximity effect correction (PEC) is, through 2D simulation, to determine the dose distribution and/or shape modification for each feature in a circuit pattern such that the written pattern is as close to the target pattern as possible. Earlier, it was shown that the 3D PEC, which considers the variation of exposure along the resist-depth dimension, would be necessary for the feature size well below 100 nm. Also, a feature-by-feature correction procedure is too time-consuming to be practical, especially for the 3D PEC of large-scale patterns. In this paper, a new method for the 3D PEC is proposed, which adopts 3D resist profile (instead of 2D exposure distribution) in optimization, but avoids the intensive computation by employing a critical-location-based correction procedure. The proposed method achieves 3D resist profiles closer to the target ones, compared to 2D PEC. The simulation results show that the proposed method has a potential to provide a practical and effective alternative to the conventional approach.
© *2011 American Vacuum Society*. [DOI: 10.1116/1.3660785]

I. INTRODUCTION

Electron-beam (e-beam) lithography plays an important role in nanofabrication, being able to transfer high-resolution patterns onto the resist. However, as the feature size decreases well below microns into nanoscale, blurring in the written pattern caused by the proximity effect due to electron scattering in the resist puts a fundamental limit on the minimum feature size and maximum circuit density that can be realized. The importance of developing effective and efficient schemes for correcting the proximity effect has been well recognized for a long time, and various methods were proposed and implemented by many researchers.[1–5] A typical approach to the proximity effect correction (PEC) employs a two-dimensional (2D) model of resist layer, i.e., the exposure (e-beam energy deposited) variation along the resist depth dimension is not taken into account. The exposures at the selected points in a circuit pattern are estimated by convolution between a circuit pattern, i.e., dose (e-beam energy given) distribution, and the point spread function (PSF), which depicts the exposure distribution throughout the resist when a single point is exposed. The amount of dose or shape adjustment for each circuit feature is determined such that a desired exposure distribution is achieved. This feature-by-feature correction procedure usually requires a long computation time.

For circuit patterns with nanoscale features, it is not unusual that the actual written pattern is substantially different from the written pattern estimated by a PEC method. One of the reasons for this deviation is that the 2D model ignores the exposure variation along the depth dimension. In an earlier study,[6] it was shown that the (remaining) resist profile estimated using a 2D model can be significantly different from the one based on a three-dimensional (3D) model, which considers the depth-dependent exposure variation. Another reason is that the actual resist profile cannot be derived directly from the exposure distribution, e.g., the developing rate is not linearly proportional to the exposure at a given point. Therefore, the PEC methods, which consider the exposure only, may suffer from substantial CD

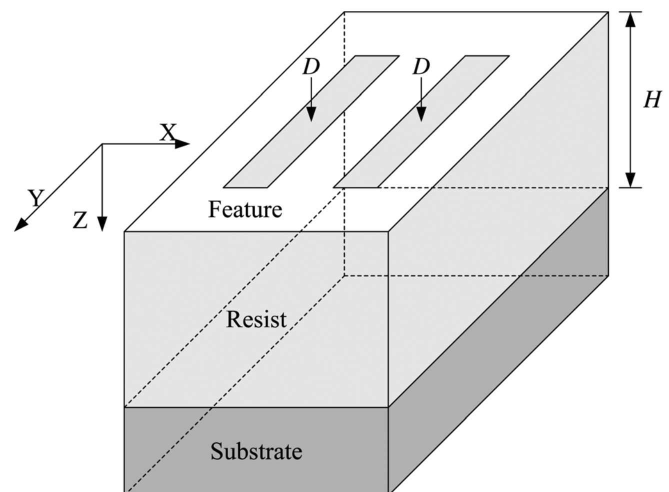

FIG. 1. Coordinates of the substrate system where H is the initial thickness of resist.

[a)]Electronic mail: jin@ucsd.edu

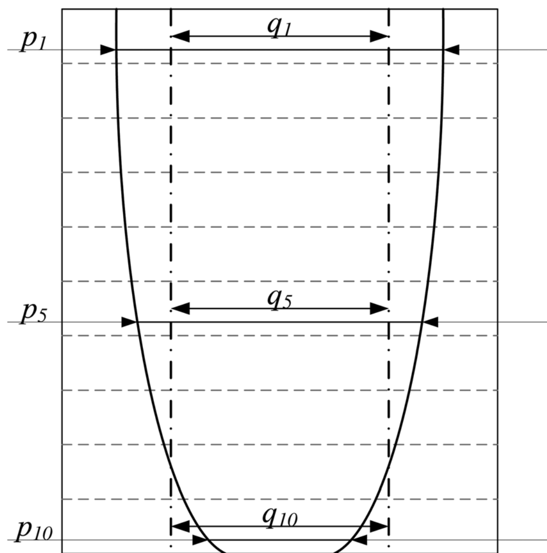

FIG. 2. Cross section of resist profile is illustrated for a line feature where p_i and q_i are the actual and target widths at the ith layer, respectively, where the resist is modeled by 10 layers. The cost function is formulated in terms of width errors at the top, middle, and bottom layers of resist.

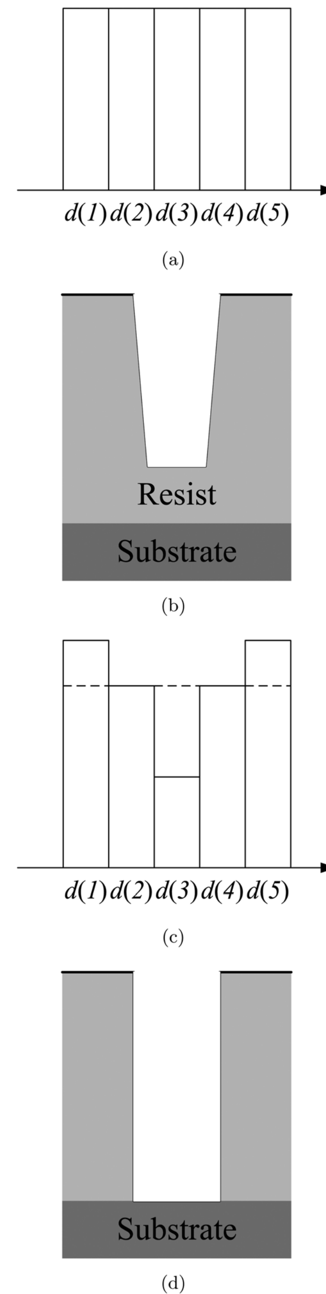

FIG. 3. Illustration of (a) the (region-wise) dose distribution within the feature before correction, (b) the corresponding resist profile before correction, (c) the (region-wise) dose distribution within the feature after correction, and (d) the corresponding resist profile after correction.

errors or deviation from the target profile in general. In addition, with a 2D model, it is not possible to consider the lateral development of resist, which affects the resist profile, in particular the sidewall shape, significantly.

In our previous studies,[6–8] the limitations of 2D PEC were analyzed and the need for 3D PEC was well demonstrated for circuit patterns with nanoscale features. In Ref. 7, the idea of true 3D PEC was proposed and its first implementation for a single line and a small number of lines was reported. In this implementation, the resist profile estimated through simulation of resist development was employed instead of the exposure distribution, in order to obtain more realistic results.

In this paper, an extension of the 3D PEC method for large-scale uniform patterns is described. A challenge is that a 3D PEC method requires a tremendous amount of computation due to the increased dimensionality and resist-development simulation. The feature-by-feature correction procedure would be too time-consuming to be practical. Hence, a new 3D PEC method has been developed, which cuts down the required computation greatly and still achieves the resist profile closely matched to the target one. It explicitly corrects the features only at the critical locations in a circuit pattern and employs a fast correction procedure for other features exploiting the uniformity of feature distribution. A distinct aspect of the method is that it attempts to adjust the exposures across (inside and outside) the feature boundary in order to control the location and shape of sidewall in the resist profile.

The rest of the paper is organized as follows. The exposure and development models are described in Sec. II. The 2D and 3D correction methods are briefly reviewed in Sec. III. The proposed 3D correction procedure is described in detail in Sec. IV. Simulation results are discussed in Sec. V., followed by a summary in Sec. VI.

II. MODELS

A. Exposure model

The substrate system consists of a substrate and a certain type of resist with initial thickness of H on top of the substrate, as illustrated in Fig. 1, where the resist depth is along the Z-dimension. The 3D point spread function is denoted by $psf(x, y, z)$, which describes the exposure distribution in the resist when a point on the X–Y plane is exposed. Let $d(x, y, 0)$ represent the e-beam dose given to the point $(x, y, 0)$ on the surface of the resist for writing a circuit feature or pattern (refer to Fig. 1):

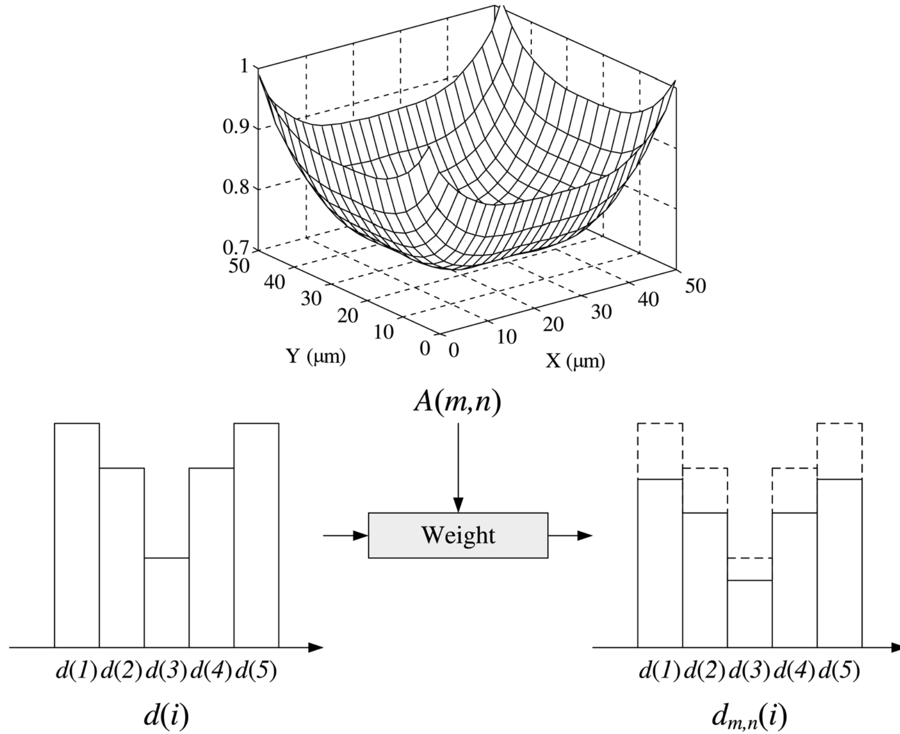

FIG. 4. For each location (m,n) of the feature (line segment), $d(i)$ is weighted by the deconvolution surface $A(m,n)$.

$$d(x,y,0)=\begin{cases} D & \text{if } (x,y,0) \text{ is within a feature} \\ 0 & \text{otherwise} \end{cases}, \tag{1}$$

where D is a constant dose.

Let us denote the exposure at the point (x, y, z) in the resist by $e(x, y, z)$. Then, the 3D spatial distribution of exposure can be expressed by the following convolution:

$$e(x,y,z)=\iint d(x-x',y-y',0)psf(x',y',z)dx'dy'. \tag{2}$$

From Eq. (2), it can be seen that the exposure distribution at a certain depth z_0 can be computed by the 2D convolution between $d(x, y, 0)$ and $psf(x, y, z_0)$ in the corresponding plane $z = z_0$, i.e., $e(x, y, z)$ may be estimated layer by layer. Note that the *PSF*, $psf(x, y, z)$, reflects all the phenomena affecting energy deposition including the e-beam blur.

B. Development model

Although the 3D exposure model provides the complete information on how electron energy is distributed in the resist, it does not directly depict the remaining resist profile after development. Therefore, it is necessary to take the resist development process also into account in order to obtain a realistic correction result. In this study, a simplified version of the resist development method ("cell removal method"), PEACE,[9] is used to derive the remaining resist profiles for comparison purposes. In this model, the resist layer is partitioned into cubic cells, and the exposure is estimated at each cell. Then the developing rate $r(x, y, z)$ of each cell is calculated from its corresponding exposure $e(x, y, z)$ through a nonlinear exposure-to-rate conversion formula, which is experimentally determined and given by

$$\begin{aligned} r(x,y,z) &= F[e(x,y,z)] \\ &= 3700\exp\left[-\left(\frac{e(x,y,z)-1.0\times10^{11}}{5.6\times10^{10}}\right)^2\right] \\ &\quad -80\exp\left[-\left(\frac{e(x,y,z)-9.0\times10^{9}}{9.0\times10^{9}}\right)^2\right]-123, \end{aligned} \tag{3}$$

where $r(x, y, z)$ is in nanometer per minute and $e(x, y, z)$ in electron volts per square micrometer.

Through iterations, the remaining time for complete development of each of the cells exposed to the developer is updated. The simulation continues for a specified developing time to obtain the final remaining resist profile.

III. CORRECTION METHODS

Let us assume that a target written pattern is specified by the corresponding resist profile (e.g., line widths at the top, middle, and bottom layers) and the cross section of resist profile is in the X–Z plane (refer to Fig. 1). During correction, at each location (x, y) in a circuit pattern, the cross-section of resist profile needs to be examined. Then, $e(x, y, z)$ and $r(x, y, z)$ can be replaced by $e(x, z)$ and $r(x, z)$, respectively.

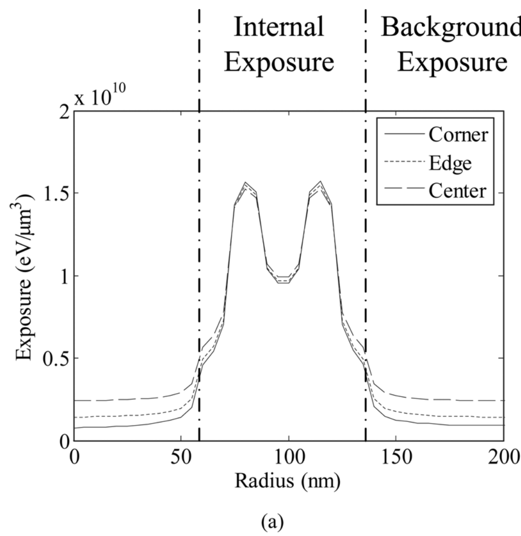

(a)

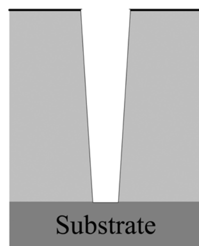

(b)

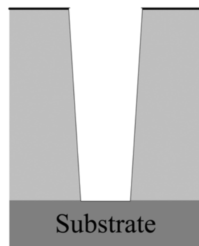

(c)

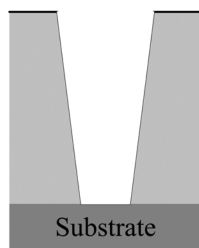

(d)

FIG. 5. (a) Exposure distributions obtained using the global (weighted) dose distribution; and the corresponding resist profiles at (b) corner, (c) edge, and (d) center of the pattern.

A. 2D exposure correction (2D PEC)

In the 2D exposure model, the exposure is assumed not to vary along the depth dimension (*Z*-dimension), i.e., $e(x, z)$ in the cross section is averaged over $0 \leq z \leq H$ (refer to Fig. 1), resulting in $e(x)$. Let $h(x)$ represent the depth distribution (i.e., depth at x) in the target resist profile. A target exposure distribution $E_t(x)$ is derived from $h(x)$ by

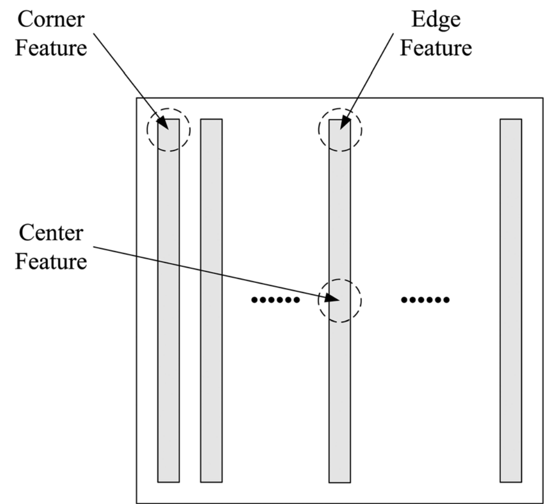

FIG. 6. Line segments only at the critical locations of the pattern are corrected individually.

$$E_t(x) = F^{-1}\left[\frac{h(x)}{T}\right], \tag{4}$$

where T is the developing time.

The exposure $E_t(x)$ can be considered as a threshold for a certain point to be fully developed. Then, the dose distribution $d(x)$ required to achieve the target resist profile (depth distribution) $h(x)$ may be determined iteratively by minimizing the following error:

$$\text{Error} = \sum_x |e(x) - E_t(x)|. \tag{5}$$

In each iteration, $e(x)$ is computed from $d(x)$ according to Eq. (2). The objective of this 2D correction scheme is to control the dose distribution $d(x)$ such that $e(x)$ is as high as the threshold $E_t(x)$ in the exposed area, and as low as possible in the unexposed area.

B. 3D resist profile correction

Unlike the above 2D exposure correction, this 3D correction incorporates the estimation of the remaining resist profile into the correction procedure and utilizes the resist profile to determine the dose distribution based on a 3D model. The overall correction procedure is very similar to that of the 2D correction. However, the error, which is to be minimized determining the corrected dose distribution, is computed based on the estimated remaining resist profile rather than the exposure distribution, and is given by

$$\text{Error} = \max_z |p(z) - q(z)|, \tag{6}$$

where $p(z)$ and $q(z)$ denote the width distribution of the estimated remaining resist profile and that of the target resist profile, respectively (refer to Fig. 2).

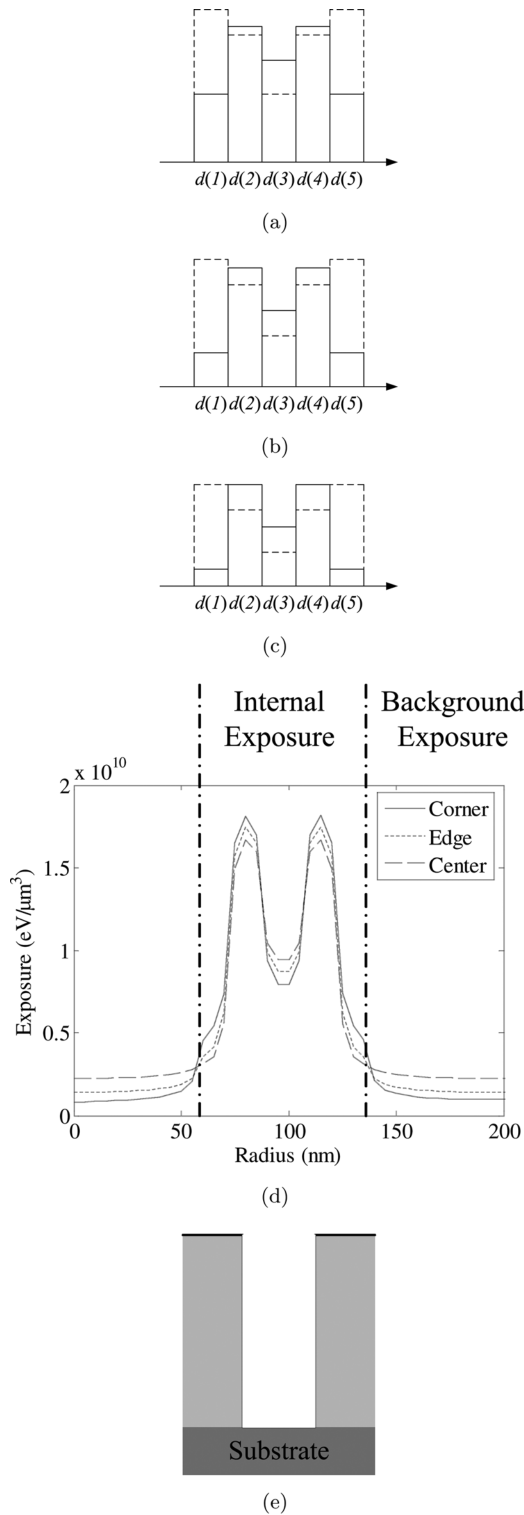

FIG. 7. Adjusted dose distributions for (a) corner, (b) edge, (c) center of the pattern, (d) the corresponding exposure distributions, and (e) the corrected resist profile (illustration).

IV. PROPOSED CORRECTION PROCEDURE (3D PEC)

The proposed 3D PEC method minimizes the deviation of resist profile from the target profile, avoiding the feature-by-feature correction without sacrificing the correction quality.

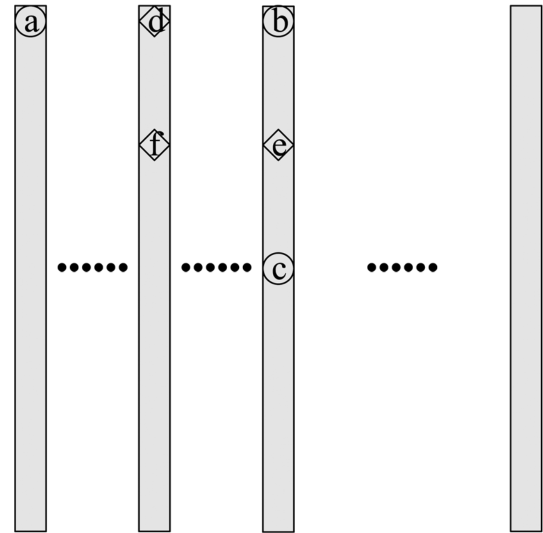

FIG. 8. Critical locations (marked by ○) and test locations (marked by ◇) in the line pattern.

It consists of three steps: correcting a single feature in isolation, global adjustment of feature-wise dose, and intrafeature dose control at critical locations.

A. Correction of a single feature

In the first step of the proposed approach, a single instance of the repeated feature in the pattern is corrected in isolation. The feature is partitioned into regions, each of which a dose is determined using the 3D resist profile correction (refer to Sec. IV B).

In the current implementation, the error defined in Eq. (6) is computed only considering the top, middle, and bottom layers of resist. The maximum of the three errors is minimized such that a profile as close to the target resist profile as possible is obtained. The (region-wise) dose distributions along with the resist profiles before and after correction are illustrated for a line feature partitioned into five regions in Fig. 3. The dose distribution within the feature is denoted by $d(i)$ and the corresponding exposure distribution by $e(i)$, where i is the region index (refer to Fig. 3). The spatial averages of $d(i)$ and $e(i)$ are denoted by D and E, respectively, i.e., $D = (1/R)\sum_{i=1}^{R} d(i)$ and $E = (1/R)\sum_{i=1}^{R} e(i)$, where R is the number of regions. Note that all of the notations, $d(i)$, $e(i)$, D, and E (i.e., without subscripts) are for a single feature in isolation.

B. Feature-wise global adjustment

In the second step, the global distribution of feature-wise dose throughout the pattern is derived by the following deconvolution:

$$A = E_t \otimes^{-1} psf, \quad (7)$$

where $E_t(m, n)$ is the target (average) exposure for the m, nth location of the feature and is assigned the value of E (see

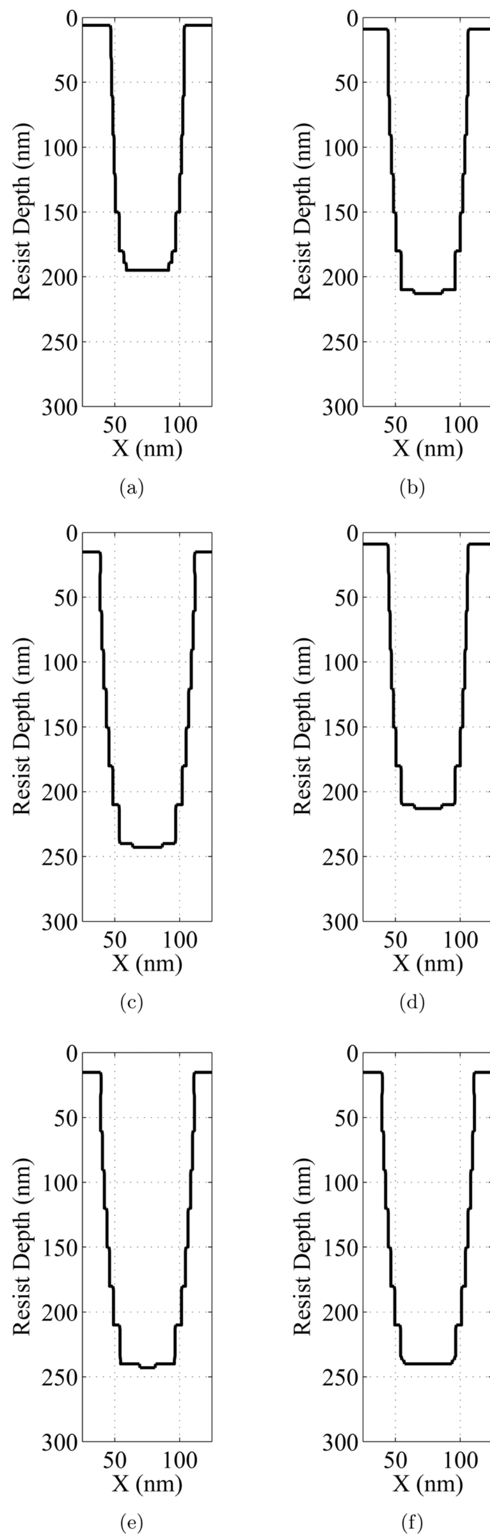

FIG. 9. Cross-section resist profiles without correction (i.e., uniform dose) at the critical locations [(a) corner, (b) edge, and (c) center; refer to Fig. 8] and the test locations [(d)–(f); refer to Fig. 8].

Sec. IV A), and *psf* is the normalized point spread function (refer to Sec. IV A) sampled at the feature interval.

The output of the deconvolution, i.e., matrix A, which specifies the (average) feature-wise dose distribution required to achieve E at all locations of the feature, is referred to as *deconvolution surface*. This deconvolution is not computationally intensive as the spatial resolution involved is coarse (feature size). For the m, nth location of the feature, $d(i)$ is weighted (scalar multiplication) by the deconvolution surface A to results in (refer to Fig. 4):

$$d_{m,n}(i) = d(i) \cdot A(m,n). \tag{8}$$

The spatial average of $d_{m,n}(i)$ is denoted by $D_{m,n}$. Now, $e_{m,n}(i)$, corresponding to $d_{m,n}(i)$, is well balanced to be E throughout the pattern, but the exposure in the unexposed area (refer to as *background exposure*) may vary with location [refer to Fig. 5(a)]. Then, as illustrated in Fig. 5, the resist profiles at different locations would be different. This variation is due to the difference in the background exposure even though the internal exposure is equalized by the deconvolution surface. In order to achieve the resist profile throughout the pattern, one may further adjust the internal exposure to compensate for the difference in the background exposure among locations.

C. Critical-location-based dose control

In a large-scale uniform pattern, the same feature such as line, square, etc. is replicated uniformly throughout the pattern. Then, the global spatial distribution of exposure is smooth, and, in turn, the global distribution of feature-wise dose required for proximity effect correction must be smooth, which is indicated by the deconvolution surface (refer to Sec. IV B). Therefore, it is sufficient to consider only the features at the *critical locations*, e.g., corner, edge, and center (refer to Fig. 6) instead of a feature-by-feature correction. Therefore, in the third step, $d_{m,n}(i)$ at each of the three critical locations is adjusted based on the same scheme in Sec. IV A. One difference is that the background exposure at each critical location, which is computed by using the deconvolution surface (refer to Sec. IV B), should be considered in the iterative correction. For each critical location, the total exposure is the sum of the base exposure and the background exposure, where the base exposure depends on $d_{m,n}(i)$ within each iteration, and the background exposure only depends on $D_{m,n}$, i.e., constant among iterations. As the resist profile after the second step is already close to the target one, $d_{m,n}(i)$ can be used as an initial distribution in order to minimize the number of iterations. The corrected dose distributions at the critical locations are illustrated in Fig. 7 and the corresponding exposure distributions in Fig. 7(d). Achieving the identical exposure distribution at all locations in a large pattern, which is attempted by most of the conventional PEC methods, would be extremely difficult if not impossible. The proposed correction method let the difference in the internal exposure compensate for that in the background exposure such that the deviation from the target profile is minimized at the critical locations [refer to Fig. 7(e)]. After the final $d_{m,n}(i)$ is obtained at each critical location, a 2D global interpolation is employed to compute the $d_{m,n}(i)$ at all other locations according to the deconvolution surface.

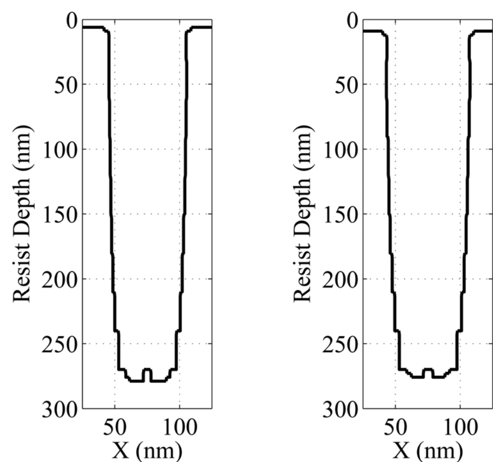

(a) (b)

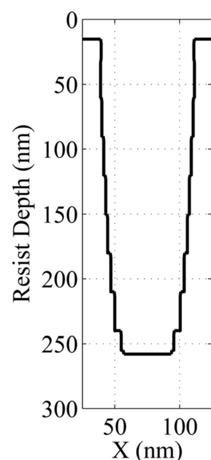

(c)

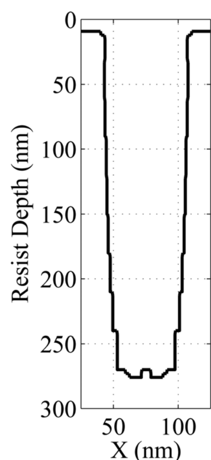

(d)

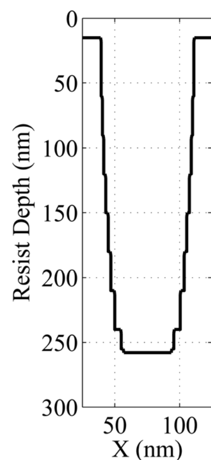

(e)

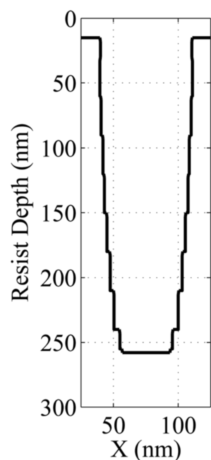

(f)

FIG. 10. Cross-section resist profiles achieved by 2D PEC method at the critical locations [(a) corner, (b) edge, and (c) center; refer to Fig. 8] and the test locations [(d)–(f); refer to Fig. 8].

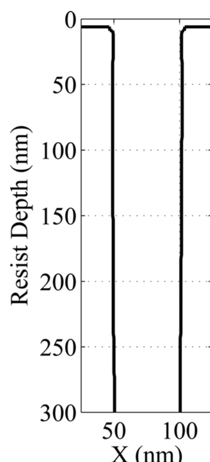

(a)

(b)

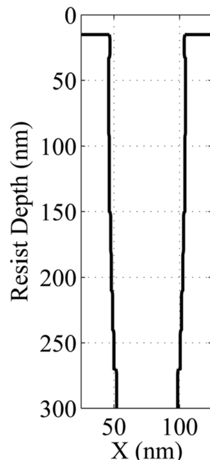

(c)

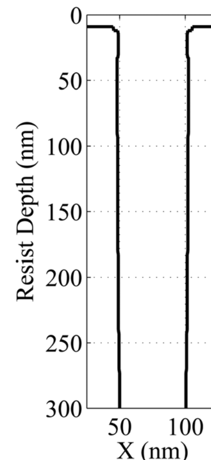

(d)

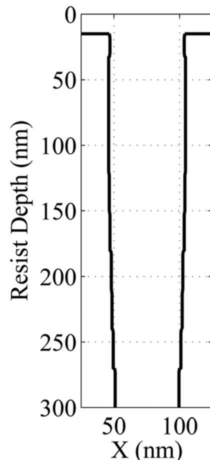

(e)

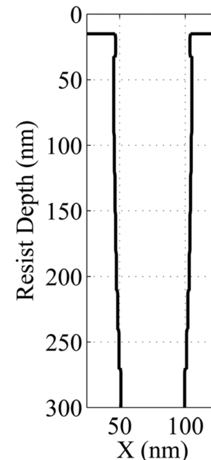

(f)

FIG. 11. Cross-section resist profiles achieved by 3D PEC method at the critical locations [(a) corner, (b) edge, and (c) center; refer to Fig. 8] and the test locations [(d)–(f); refer to Fig. 8].

V. RESULTS AND DISCUSSION

The proposed approach to 3D proximity effect correction for large-scale uniform patterns has been implemented and its performance has been analyzed through simulation.

A. Patterns

Two kinds of the uniform pattern consisting of lines shown in Fig. 8 were employed for performance analysis. In the one, to be referred to as Pattern I, each line is 51 μm long

TABLE I. Average and maximum percent width errors in resist profiles for no correction, 2D PEC method, and 3D PEC method.

Simulation settings		No correction		2D PEC method		3D PEC method	
PMMA thickness (nm)	Pattern	Average (%)	Maximum (%)	Average (%)	Maximum (%)	Average (%)	Maximum (%)
100	I	5.20	12.33	4.40	8.33	2.33	4.33
	II	1.12	1.67	0.50	1.08	0.32	1.00
300	I	44.39	100.00	36.07	94.33	8.70	13.17
	II	13.90	32.27	10.00	17.00	2.57	4.42
500	I	69.08	100.00	65.45	100.00	41.30	60.33
	II	45.85	100.00	33.88	100.00	9.50	13.58

and 50 nm wide, and the gap between lines is 50 nm. In the other pattern, to be referred to as Pattern II, each line is 51 μm long and 100 nm wide, and the gap between lines is 100 nm. Both patterns cover the full range of electron scattering (for 50 keV). The correction program partitions each line into segments of 3 μm for dose control. The three critical and three test locations are shown in Fig. 8.

B. Simulation results

The PSF's employed in the simulation are generated by a Monte Carlo simulation method, SEEL.[10] The substrate systems employed in the simulation are composed of PMMA (Poly(methyl methacrylate)) on Si, where the three different PMMA thicknesses, 100, 300, and 500 nm, are considered. The beam energy is set to 50 keV with the beam diameter of 5 nm. These three substrate systems along with the two patterns provide six different combinations so that the proposed approach can be thoroughly tested. The patterns were corrected by the 2D PEC (refer to Sec. IV A) and (propose) 3D PEC methods for the target resist profile of vertical sidewall. No correction (a uniform dose for all features), the 2D PEC method and the 3D PEC method are compared with a constraint that the total dose for a pattern must be the same for all the methods. The results (cross-section resist profiles) of pattern I for 300 nm PMMA on Si are provided in Figs. 9–11. From the profiles obtained without correction (Fig. 9), it can be seen that the resist profile significantly varies with location. The linewidth is not uniform and the sidewall is clearly of overcut. A distinct aspect of the 3D PEC method is that it explicitly equalizes the resist profile (rather than the exposure) of a feature throughout a pattern. Although the resist profiles (Fig. 10) obtained by the 2D PEC method are better than those without correction, the variation of resist profile among locations is still substantial. However, as can be seen in Fig. 11, the proposed 3D PEC method greatly improves the uniformity of resist profile among not only the critical locations, but also the test locations, and also achieves the resist profiles much closer to the target one in terms of linewidth and sidewall type (vertical).

The correction methods are also compared quantitatively in terms of the percent width errors (refer to Sec. III) as follows:

$$\text{Average Percent Width Error} = \frac{1}{n}\sum_{j=1}^{n}\frac{|p'(j)-q(j)|}{q(j)} \times 100\%, \tag{9}$$

$$\text{Max Percent Width Error} = \max_{j=1}^{n}\frac{|p'(j)-q(j)|}{q(j)} \times 100\%, \tag{10}$$

where $p'(j)$ is the width of the jth layer in the final resist profile after correction, $q(j)$ is the target profile as defined in Sec. IV A., and n is the number of resist layers.

The average and maximum percent width errors are provided in Table I. Note that the maximum error reaches 100% in some cases, due to the underdevelopment in resist profiles (e.g., the bottom layer is not developed at all, leading to a zero width). The results show that the errors for the 2D PEC method are significantly smaller than those when no correction is done (i.e., a uniform dose). More importantly, compared to the 2D PEC method, the proposed 3D PEC method further reduces both average and maximum errors greatly.

From Table I, it is observed that as the resist thickness increases, the improvement (reduction in the total percent errors) by the proposed method becomes larger. For a thicker resist, the exposure variation along the depth dimension is larger, which makes the 2D PEC method suffer from larger errors as it ignores the variation. Also, the increase of exposure variation makes the resist profile more sensitive to the dose distribution. Therefore, incorporating the estimation of remaining resist profile into the correction procedure can achieve a more realistic correction, which lacks in the 2D PEC method. When the feature size decreases, the improvement by the proposed method tends to be larger (except for the resist thickness of 500 nm). For the same substrate system, a smaller feature is affected relatively more by the proximity effect and the development process; therefore a larger room for improvement. However, for a very thick resist, the proximity effect correction itself becomes harder for a smaller feature.

VI. SUMMARY

A new practical method for true 3D proximity effect correction, which can handle large-scale uniform patterns efficiently, has been developed. It performs real 3D PEC by taking into account the exposure variation along the resist depth dimension (in addition to the lateral dimensions). The cost (error) function employed in correction is not the conventional (2D) CD error, but the 3D CD error, i.e., the CD errors at multiple layers of resist are considered. Also, the method incorporates the resist development simulation into the correction procedure to achieve realistic results. In order to alleviate the computational requirement for large-scale patterns, a critical-location-based correction approach is taken along with the deconvolution surface for deriving the corrected doses for other locations. Through the extensive simulation, it has been shown that the proposed 3D PEC method can significantly improve correction results, compared to the 2D PEC method, in terms of resist profile, i.e., not only the CD error but also the sidewall shape. A future effort will be on extending the 3D PEC method for nonuniform large-scale patterns.

ACKNOWLEDGMENT

This work was supported by a research grant from Samsung Electronics Co., Ltd.

[1] R. Rau, J. McClellan, and T. Drabik, J. Vac. Sci. Technol. B **14**, 2445 (1996).
[2] S.-Y. Lee and B. D. Cook, IEEE Trans. Semicond. Manuf. **11**, 108 (1998).
[3] C. S. Ea and A. D. Brown, J. Vac. Sci. Technol. B **17**, 323 (1999).
[4] K. Takahashi, M. Osawa, M. Sato, H. Arimoto, K. Ogino, H. Hoshino, and Y. Machida, J. Vac. Sci. Technol. B **18**, 3150 (2000).
[5] M. Osawa, K. Takahashi, M. Sato, H. Arimoto, K. Ogino, H. Hoshino, and Y. Machida, J. Vac. Sci. Technol. B **19**, 2483 (2001).
[6] S.-Y. Lee and K. Anbumony, Microelectron. Eng. **83**, 336 (2006).
[7] K. Anbumony and S.-Y. Lee, J. Vac. Sci. Technol. B **24**, 3115 (2006).
[8] S.-Y. Lee and K. Anbumony, J. Vac. Sci. Technol. B **25**, 2008 (2007).
[9] Y. Hirai, S. Tomida, K. Ikeda, M. Sasago, M. Endo, S. Hayama, and N. Nomura, IEEE Trans. Comput.-Aided Des. **10**, 802 (1991).
[10] S. Johnson, "Simulation of electron scattering in complex nanostructures: Lithography, metrology, and characterization," Ph.D. dissertation, Cornell University, Ithaca, NY, 1992.